Zeeman Effect of No-Phonon $^4A_{2g}$-$^4T_{2g}$ Transition of Cr^{3+} in TiO_2

Ludwig Grabner
National Bureau of Standards, Washington, D. C. 20234
Eugene Y. Wong
Physics Department, University of California, Los Angeles, California 90024
(Received 2 April 1973)

The site symmetry of Cr^{3+} in TiO_2 is D_{2h} which splits the cubic (O_h) $^4T_{2g}$ state into $^4B_{1g}$, $^4B_{2g}$, and $^4B_{3g}$. Spin-orbit interaction further splits these states into six Kramers doublets all of symmetry Γ_5^+. Previous optical work on TiO_2: Cr^{3+} established the lowest-lying sharp lines at 12 685 and 12 732 cm^{-1} as no-phonon lines of magnetic dipole character. It proposed these lines as due to transitions between the $^4A_{2g}$ ground state and two of the above six states. The present report extends this work by a Zeeman study, in emission, at 4 K of the line at 12 685 cm^{-1}. The results are: The Zeeman splitting of this line identifies the excited state of this transition as the $M_s = \pm 3/2$ spin-orbit component of an orbital state consisting of 77% $^4B_{2g}$, 17% $^4B_{1g}$, and 6% $^4B_{3g}$ with an effective $g = 1.73$. Furthermore, the line at 12 732 cm^{-1} is identified as the $M_s = \pm 1/2$ spin-orbit component by its effect in second order in the magnetic field on the Zeeman pattern of the line at 12 685 cm^{-1}. For the excited state the spin is quantized along the x direction of the magnetic axes while for the ground state it is quantized along the z direction. The reason for spin quantization along the x axis is discussed.

INTRODUCTION

The purpose of this paper is to extend previous work[1] on the spectroscopy of Cr^{3+} in TiO_2 to the determination of the character of the lowest excited state. Figure 1 reproduces from Ref. 1 an absorption spectrum showing two sharp no-phonon lines A_- (12 685 cm^{-1}) and A_+ (12 732 cm^{-1}), which were shown to be magnetic dipole transitions. Our aim is the identification of the lowest excited state by studying the Zeeman effect on the line A_-. Reference 1 suggested that this state is possibly of $^4T_2$ origin rather than the usual ^2E and the reasons for proposing this assignment can be found there. If this is indeed the case, then Cr^{3+} in TiO_2 is unique in that the $^4A_2 \leftrightarrows {}^4T_2$ transition show not only broadband spectra,[2] but features *line spectra* in addition. In fact, it is just this feature which enables a Zeeman study which, for this reason, has so far been confined to $^4A_2 \leftrightarrows {}^2E$ and $^4A_2 \leftrightarrows {}^2T_2$ transitions.[3,4]

The rutile structure of TiO_2 is a tetragonal crystal belonging to the crystal class D_{4h} and the space group D_{4h}^{14} ($P4_2/mnm$). The unit cell (Fig. 2) contains six atoms. Each Ti^{4+} is surrounded by a slightly deformed oxygen octahedron, so that the local symmetry of a Ti^{4+} site is only orthorhombic (D_{2h}). There are two Ti^{4+} sites in the unit cell which are related by a rotation of 90° around the c axis of the crystal. These sites, which are equivalent without a magnetic field, will be referred to as sites A and B, respectively. The electron paramagnetic resonance spectrum has been studied by Gerritsen and co-workers[5] who find that in Cr-doped TiO_2 almost all the Cr^{3+} ions are in Ti^{4+} substitutional sites with no local charge compensation. The site symmetry of D_{2h} splits the cubic $^4T_{2g}$ state into $^4B_{1g}$, $^4B_{2g}$, and $^4B_{3g}$ states (notation Tinkham[6]). Spin-orbit interaction further splits these states into six Kramers doublets all of symmetry Γ_5^+, each of which can be regarded as a suitable mixture of $^4B_{1g}$, $^4B_{2g}$, and $^4B_{3g}$ states. With the help of the EPR data of Gerritsen *et al.* we will show that the lines A_- and A_+ (Fig. 1) are, in fact, due to $^4A_2 \rightleftarrows {}^4B_2$ ($\pm\frac{3}{2}$) and $^4A_2 \rightleftarrows {}^4B_2$ ($\pm\frac{1}{2}$) transitions, respectively. This confirms the conjecture of Ref. 1 that the lowest excited states originate in the $^4T_2$ state by identifying two of its components as $\pm\frac{3}{2}$ and $\pm\frac{1}{2}$ states with an orbital part consisting mainly of the B_2 state.

RESULTS AND ANALYSIS

The samples of single-crystal TiO_2 : Cr^{3+} used are identical with those used in Ref. 1. The concentration of Cr^{3+} was not sufficient to give enough contrast on the photographic plate when the crystals were studied in absorption. Consequently, the Zeeman effect was studied in emission using the 4880-Å line of an argon laser as exciting radiation. A 2-m grating Ebert spectrograph was used and a superconducting magnet provided the magnetic field. The results are shown in Figs. 3 and 4; the captions summarize the condition of observation. All measurements are at 4 K.

A. $\vec{H} \parallel \hat{c}, \vec{k} \parallel \hat{a}$

We shall first analyze the Zeeman spectrum (Fig. 3) for the case when $H = 39$ kG is parallel to the c axis (y axis) and the emission is observed along the a axis. The axes are defined in Fig. 2. The two Cr^{3+} ions of the unit cell are equivalent when H is

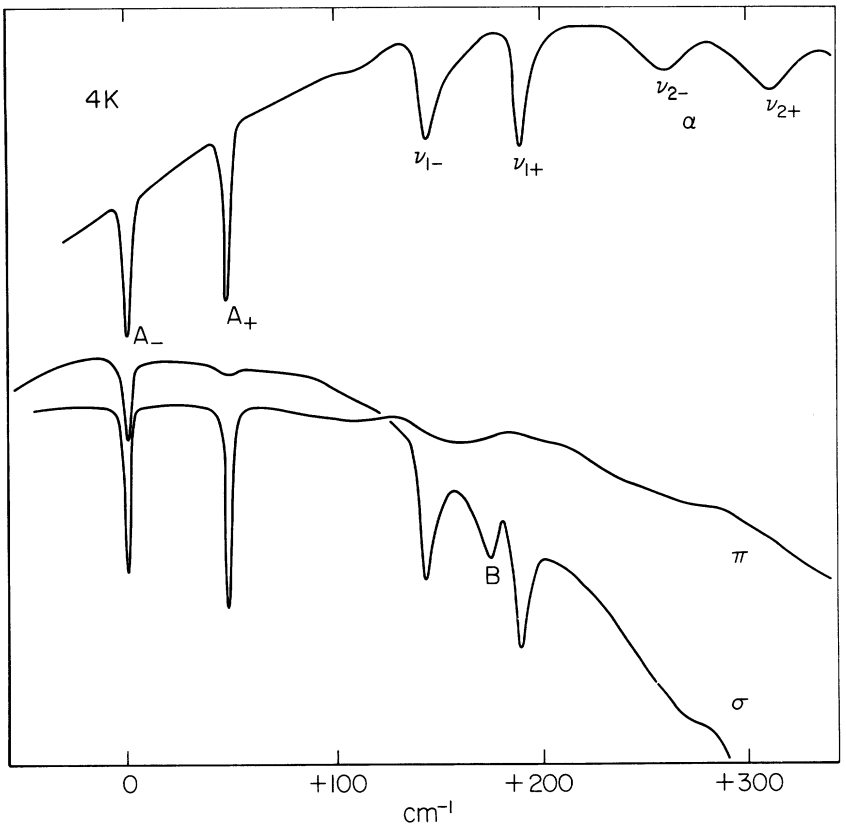

FIG. 1. Absorption spectrum of TiO_2: 0.02-at.% Cr at 4 K near no-phonon transitions A_- (12685 cm^{-1}) and A_+ (12732 cm^{-1}) in α, π, and σ polarizations. The ordinate represents transmission. ν_{1-}, ν_{1+}, and ν_{2-} and ν_{2+} are phonon side-bands of the no-phonon lines A_- and A_+, respectively. In present work, Zeeman effect on lines A_- in emission is studied. Reproduction of Fig. 5 of Ref. 1.

in the *ac* plane and, therefore, for $\vec{H} \parallel \hat{c}$. Referred to the axes of Fig. 2, the $^4A_2$ ground state is described by the spin Hamiltonian

$$\mathcal{H} = \mu_B H g S + D[S_z^2 - \tfrac{1}{3}S(S+1)] + E(S_x^2 - S_y^2),$$

with $g = 1.97$, $D = -0.68$ cm^{-1}, and $E = 0.14$ cm^{-1}.[5] When $H_y = 39$ kG the first term is the largest. When the spin is quantized in the *y* direction, second-order perturbation theory, in which the *D* and *E* terms are used as a perturbation, gives the following eigenvalues of the spin Hamiltonian: $E_{3/2}$, $E_{1/2}$, $E_{-1/2}$, and $E_{-3/2}$ equal 5.95, 1.27, −2.36, and −4.86 cm^{-1}, respectively. Transitions to these four states from a single excited state would result in four lines with separations of 4.68, 3.63, and 2.49 cm^{-1}, respectively. This is in agreement with the data shown in Fig. 3 from which we conclude that, indeed, the excited state is not split by a magnetic field. The $M_s = \pm\frac{1}{2}$ states, whether $S = \frac{1}{2}$ or $\frac{3}{2}$, will split in a magnetic field irrespective of axis of quantization. On the other hand, the $M_s = \pm\frac{3}{2}$ states will not split to first order in *H* if they are quantized perpendicular to the magnetic field. We, therefore, conclude that the excited state is a $M_s = \pm\frac{3}{2}$ state quantized perpendicular to the magnetic field, i.e., it is subject to a crystal field $D[S_z^2 - \frac{1}{3}S(S+1)] + E(S_x^2 + S_y^2)$, with $D \gg E$ and $D \gg \mu_B H$.

Previous work[1] established the transition as magnetic dipole. According to Sugano and coworkers,[7] when spin-orbit interaction is neglected, the magnetic dipole transitions between the $^4A_2$ ground state and the $^4T_2$ excited state are determined by the matrix element $\langle {}^4A_2 | \vec{M} | {}^4T_2 \rangle$, with $\vec{M} = \vec{L} + 2\vec{S}$. Since spin-orbit interaction is neglected, spin is conserved in the transition. Because of small-*D* and -*E* terms, the ground-state

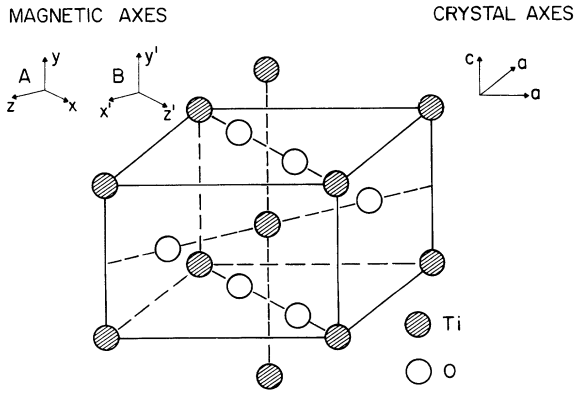

FIG. 2. Rutile structure. There are two Ti^{4+} sites in the unit cell related by a rotation of 90° around *c* axis of crystal. These are referred to as sites *A* and *B*. The magnetic axes as determined in Ref. 5 and the crystal axes are shown.

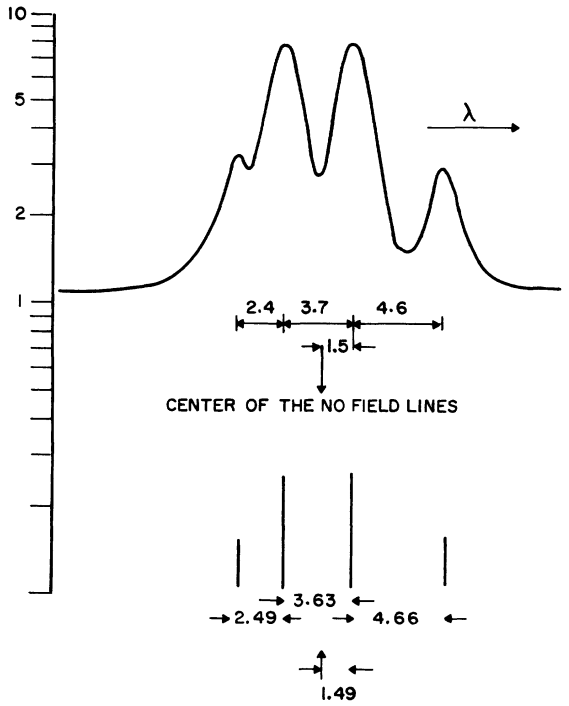

FIG. 3. Zeeman emission spectrum of line A_- (12 685 cm^{-1}) shown in absorption in Fig. 1. $H=39$ kG is parallel to the c axis (y axis) and the emission is observed along the a axis. The axes are defined in Fig. 2. Units are in cm^{-1}; $T=4$ K.

spin is quantized along the magnetic field (y direction). The excited state, on the other hand, is quantized 90° from the y direction. A transformation of axes to y-direction quantization gives $|M_{3/2}\rangle = (1/\sqrt{8})\{|\frac{3}{2}\rangle + \sqrt{3}|\frac{1}{2}\rangle + \sqrt{3}|-\frac{1}{2}\rangle + |-\frac{3}{2}\rangle\}$. One thus expects four transitions with the intensity ratio 1 : 3 : 3 : 1. This is in good agreement with the experimental data shown in Fig. 3 if the photographic plate is assumed to have a logarithmic response.

The center of the no-field line should be 1.27 cm^{-1} from the transition connecting the $M_s=\pm\frac{1}{2}$ states. According to experiment it is 1.47 cm^{-1}. But if the line A_+ (Fig. 1) at 12 732 cm^{-1} is identified as a transition from the $\pm\frac{1}{2}$ state of the $^4T_2$ parent, the second-order Zeeman effect shifts the $M_s=\pm\frac{3}{2}$ state 0.21 cm^{-1} to the red. Adding the second-order shift to 1.27 cm^{-1} gives good agreement with experiment. Thus the second-order Zeeman effect identifies the excited state of the transition giving rise to the line A_+ as a $\pm\frac{1}{2}$ state.

B. $\vec{H} \parallel [110], \vec{k} \parallel \vec{H}$

Figure 4 shows the results when $H=62$ kG is perpendicular to the c axis and 45° from the a axis and the emission is observed along H. In this case, the two sites are not equivalent. For site A (Fig. 2), $\vec{H} \parallel \hat{z}$ and $\vec{k} \parallel \hat{x}$ and for the ground-state Zeeman energies $E_{3/2}$, $E_{1/2}$, $E_{-1/2}$, and $E_{-3/2}$, we calculate 7.87, 3.53, −2.17, and −9.23 cm^{-1}, respectively. For site B, $\vec{H} \parallel \hat{x}'$ and $\vec{k} \parallel \hat{z}'$; $E_{3/2}$, $E_{1/2}$, $E_{-1/2}$, and $E_{-3/2}$ are 8.72, 2.74, −3.02, and −8.44 cm^{-1}, respectively. As in case A, the axis of quantization is along $\vec{H}$ and the D and E terms of the spin Hamiltonian are taken into account using second-order perturbation theory. Transitions from an unsplit excited state to the four Zeeman levels of site A would result in four lines with an intensity ratio of 1 : 3 : 3 : 1 separated by 7.06, 5.70, and 4.34 cm^{-1}. In agreement with the above, we find (Fig. 4) separations (without the center line) of 7.08, 5.62, and 4.29 cm^{-1}. At 62 kG the second-order Zeeman shift due to the perturbation of the $M_s=\pm\frac{3}{2}$ state by the $M_s=\pm\frac{1}{2}$ state gives a red shift of 0.53 cm^{-1}, which just accounts for the shift of the Zeeman pattern from the center of the no-field line.

One of the lines of Fig. 4 is too strong to support the expected intensity ratio of 1 : 3 : 3 : 1. However, it may be a superposition of a line from site A and site B. When H is parallel to the z or y direction for site A, experiment shows that the excited state does not split. Thus, it must split when $\vec{H} \parallel \hat{x}'$ as is the case with site B. Then both the excited state and the ground state are quantized along H. Conservation of spin then only gives two lines one of which, in superposition with a line from site A, accounts for the large intensity of the strong central line. The separation of the central line and the center of the no-field line gives a $g=1.73$ for $M_s=\pm\frac{3}{2}$.

Summarizing, the Zeeman effect (Figs. 3 and 4) of the line A_- (Fig. 1) demonstrates that it is due to a transition from an excited state $M_s=\pm\frac{3}{2}$ and that the excited state of line A_+ (Fig. 1) is an $M_s=\pm\frac{1}{2}$ state. Both are quantized along the x axis (Fig. 2). It should be noted that the $^4A_2$ ground state is quantized along the z axis.

The $M_s=\pm\frac{3}{2}$ and $M_s=\pm\frac{1}{2}$ states above must be spin-orbit components of a quartet state. Its orbital character is secured as T_2 rather than T_1 by observing that for all values of the crystal field the $^4T_2$ state lies lower in energy than the $^4T_1$ state as shown by an inspection of the Tanabe-Sugano[8] term diagram for octahedral d^3 complexes.

C. Polarization of the Zeeman Spectrum

Neglecting spin-orbit interaction, the $^4T_{2g}$ term splits into three components, $^4B_{1g}$, $^4B_{2g}$, and $^4B_{3g}$, under a crystal field of symmetry D_{2h}. The spin-orbit interaction mixes these three states giving rise to the only irreducible representation of the double group D_{2h}, Γ_5^+. Since B_1, B_2, and B_3 transform as does L_x, L_y, and L_z, respectively, and the polarization is due to the orbital part of the wave function, the amount of mixing can be determined from polarization studies of the Zeeman spectrum.

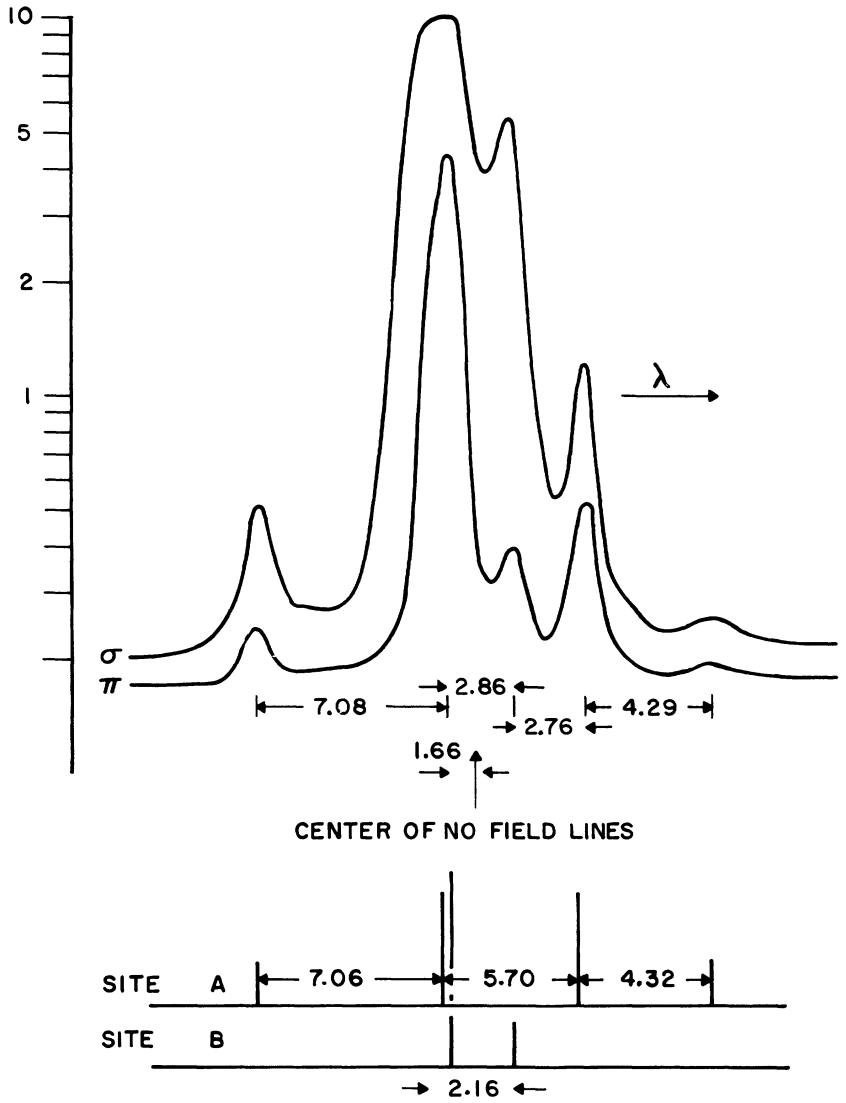

FIG. 4. Zeeman emission spectrum of line A_- (12 685 cm^{-1}) shown in absorption in Fig. 1. $H=62$ kG is perpendicular to c axis and the angle between H and a axis is 45°. Emission is observed along H. The axes are defined in Fig. 2. Units are in cm^{-1}; $T=4$ K.

The α polarization measures the magnetic dipole along the y axis for both site A and B, while the π polarization measures the magnetic dipole along the x direction for site A and the y direction for site B. The photographic plate was not calibrated but assuming a logarithmic response and integrating the densitometer trace shown in Fig. 4, a rough estimate of the intensity ratio can be obtained. The excited state identified this way has 77% $^4B_{2g}$, 17% B_{1g}, and 6% $^4B_{3g}$, with $M_s=\pm\frac{3}{2}$ at 12 685 cm^{-1} (A_-) and $M_s=\pm\frac{1}{2}$ at 12 732 cm^{-1} (A_+). The axis of quantization is along the x direction and $g=1.73$.

DISCUSSION

A detailed discussion of the spectrum for the d^3 configuration is impossible because of limited information. However, a simple model limited to the $^4T_{2g}$ term may be useful. There are only two quartet terms of the free ion in the d^3 configuration, namely, ^4F and ^4P, and only the ^4F term gives rise to $^4T_{2g}$ in a crystal field of symmetry O_h. The wave function of the $^4T_{2g}$ term can be written in the ^4F manifold of the free-ion states as

$$|B_{1g}\rangle = (1/\sqrt{2})(U_2 - U_{-2}),$$

$$|B_{2g}\rangle = (1/\sqrt{2})\{-\sqrt{\tfrac{3}{8}}(U_3 - U_{-3}) + \sqrt{\tfrac{5}{8}}(U_1 + U_{-1})\},$$

$$|B_{3g}\rangle = (1/\sqrt{2})\{\sqrt{\tfrac{3}{8}}(U_3 - U_{-3}) + \sqrt{\tfrac{5}{8}}(U_1 - U_{-1})\}.$$

The spin-orbit interaction mixes B_{1g} and B_{3g} into B_{2g} through the operators L_xS_x and L_yS_y, respectively. Second-order perturbation theory contains the matrix-element square which provides an S_x^2 and S_y^2 term for an effective spin Hamiltonian for $^4B_{2g}$. The amount of mixing of B_1 and B_3 into B_2 is

$$\left|\lambda_{^4F}\frac{\langle {}^4B_2|L_xS_x|{}^4B_1\rangle}{E_{B_1}-E_{B_2}}\right|^2$$

and

$$\left|\lambda_{4_F}\frac{\langle {}^4B_3|L_yS_y|{}^4B_2\rangle}{E_{B_3}-E_{B_2}}\right|^2,$$

respectively. $\lambda_{4_F}=\frac{1}{3}\zeta_{3d}=92\ \mathrm{cm}^{-1}$ is the spin-orbit coupling constant for the ${}^4F$ configuration, $\zeta_{3d}=300\ \mathrm{cm}^{-1}$ is the spin-orbit coupling constant for a $3d$ electron of Cr^{3+}.[9] From the polarization data discussed previously we know that ${}^4B_1$ mixes more than ${}^4B_3$, therefore, the term containing $\vec{S}_x^2$ term and the spin will primarily be quantized in the x direction. It should be noted that for the ground state the zero-field axis of quantization is along the z axis.

The zero-field separation of the $\pm\frac{3}{2}$ state (A_-) and the $\pm\frac{1}{2}$ state (A_+) is due to the perturbation from all the states. The contribution from ${}^4B_1$ is 15 cm^{-1} and that of ${}^4B_3$ is $-2\ \mathrm{cm}^{-1}$ giving a total of 17 cm^{-1}. The experimental value is 47 cm^{-1} (see Fig. 1). In Ref. 1 (Fig. 4, insert) a splitting of 1.4 cm^{-1} of the A_- line (Fig. 1) was found in agreement with the zero-field splitting of the ground state determined in Ref. 5. The intensity ratio is about 1 : 1.2, the lower-energy line of the pair has the larger intensity. If the excited state is quantized in the x direction and the ground state in the z direction this ratio should be 1 : 3. If the nonzero E term of the ground-state Hamiltonian is taken into account this ratio is changed to 1 : 2.2. It is possible that the spin Hamiltonian of the excited state also has a small-E term that will change the ratio to the experimental value of 1 : 1.2. A small-E term will split the excited state when H is along the y or z direction by second-order perturbation. However, with a linewidth of about 2 cm^{-1} a small splitting will not be detected.

The mixing of ${}^4B_{1g}$ with ${}^4B_{2g}$ will conserve the spin in x quantization but the orbital part will produce a g shift. If the wave function is $\sin\theta\psi_{{}^4B_{2g}}+\cos\theta\psi_{{}^4B_{1g}}$, the g shift will be $\frac{1}{3}\sin\theta\cos\theta$. From the polarization data discussed previously, we know that $\sin^2\theta=0.77$ and that $\cos^2\theta=0.17$. From this we calculate a g shift of -0.12 assuming that ${}^4B_{1g}$ is above ${}^4B_{2g}$ in energy. Adding the contribution from $\sin^2\theta+\cos^2\theta=0.97$, the total g shift is -0.24 or the effective g is 1.76. Since $\langle {}^4B_{3g}|\vec{M}|{}^4B_{2g}\rangle=0$, the ${}^4B_{3g}$ component does not contribute to the g shift of ${}^4B_{2g}$.

In conclusion we wish to remark on the relevance of the defect in TiO_2, consisting of a Cr^{3+} ion at a Ti^{4+} site, to the general problem of the optical properties of defects in solids. Experience shows that most optical-absorption and emisson spectra fall roughly into two classes: line spectra or broadband featureless spectra with the latter most prevalent. Figure 5 summarizes qualitatively the well-known[10] essentials of the explanation of this experience. The critical quantity is the "displacement recoil"[11] Δ, which determines the strength of the defect-lattice interaction and the overlap[11] between the vibrational part of the total wave function of the ground and excited states, respectively. Δ is the difference in the equilibrium lattice configuration of the excited state with respect to the ground state. If these are identical, for example, as in the ${}^4A_2(d\epsilon^3)\rightleftarrows{}^2E(d\epsilon^3)$ transition of octahedrally coordinated Cr^{3+} complexes, Δ will be small and therefore the no-phonon lines will be prominent because of good overlap between vibrational wave functions of the same quantum number.[12] Furthermore, the phonon participation will be small because of the small defect-lattice interaction. On the other hand, if the ground and excited state are of different electronic configuration, the relaxation of the lattice required to adjust to the new electronic configuration immediately after a transition may be large thus inducing a large Δ. In fact, Δ may be so large that there is negligible overlap between vibrational wave functions of the same quantum number. In that case the purely electronic transition consisting of the no-phonon line is completely suppressed but the large defect-lattice interaction gives rise to multiphonon transitions resulting in a broadband which is properly regarded as a phonon sideband of the suppressed no-phonon line. Therefore, spectra consisting of broad featureless bands are due to transitions between states of different electron configuration. This is the case most frequently observed. Cr^{3+} in TiO_2 is unique in the

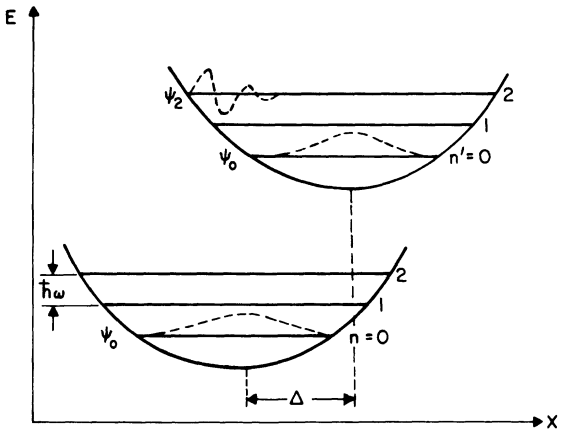

FIG. 5. Adiabatic potentials with a one-dimensional configuration coordinate model for a defect in a solid. "Displacement recoil" Δ determines the extent of no-phonon and phonon participation in a transition by the overlap of vibrational wave functions with the same or different quantum numbers, respectively. Δ also determines the coupling strength S of defect lattice $S=\omega\Delta^2/2\hbar$. S will be small or large if the electron configuration of the ground and excited state are the same or different, respectively.

spectroscopy of octahedrally coordinated Cr^{3+} complexes in providing an interesting example of an intermediate case where Δ is such that it provides sufficient defect-lattice interaction so that the multiphonon processes dominate giving rise to a broadband. However, Δ is not large enough to suppress the no-phonon lines by annulling the overlap between vibrational wave functions of the same, quantum number. It is just this fact which enables a Zeeman study of Cr^{3+} in TiO_2 showing that the excited state is of $^4T_2$ origin which has the electron configuration $d\epsilon^2 d\gamma$ different from the $^4A_2$ ground-state electron configuration $d\epsilon^3$. In the preceding remarks, to avoid complication, we have only considered the interaction of vibrational modes for which the difference between excited- and ground-state adiabatic potentials is a constant plus a term linear in the normal mode displacement. Differences in frequency between ground- and excited-state oscillators have been neglected.

[1]Ludwig Grabner, S. E. Stokowski, and W. S. Brower, Jr., Phys. Rev. B 2, 590 (1970).

[2]Leslie S. Forster, in *Transition Metal Chemistry* (Marcel Dekker, New York, 1969), Vol. 5, p. 1; H. L. Schläfer, H. Gausmann, and H. Witzke, J. Chem. Phys. 46, 1423 (1967); A. M. Glass, J. Chem. Phys. 50, 1501 (1969).

[3]Saturo Sugano and Ikuji Tsujikawa, J. Phys. Soc. Jap. 13, 899 (1958); S. Sugano, A. L. Schawlow, and F. Varsanyi, Phys. Rev. 120, 2045 (1960); D. L. Wood, W. E. Burke, and L. G. Van Uitert, J. Chem. Phys. 51, 1966 (1969); W. J. Burke and R. J. Pressley, Phys. Rev. 182, 395 (1969); Yasutaro Uesaka, Toshiro Ban, and Ikuji Tsujikawa, J. Phys. Soc. Jap. 30, 228 (1971); Naoki Koshizuka, Toshiro Ban, and Ikuji Tsujikawa, J. Phys. Soc. Jap. 30, 470 (1971).

[4]Saturo Sugano and Ikuji Tsujikawa, J. Phys. Soc. Jap. 13, 899 (1958).

[5]H. J. Gerritsen, S. E. Harrison, H. P. Lewis, and J. P. Wittke, Phys. Rev. Lett. 2, 153 (1959); H. J. Gerritsen, S. E. Harrison, and H. P. Lewis, J. Appl. Phys. 31, 1566 (1960).

[6]Michael Tinkham, *Group Theory and Quantum Mechanics* (McGraw-Hill, New York, 1964), p. 327.

[7]S. Sugano, A. L. Schawlow, and F. Varsanyi, Phys. Rev. 120, 2045 (1960).

[8]Yukito Tanabe and Saturo Sugano, J. Phys. Soc. Jap. 9, 766 (1954).

[9]Charlotte E. Moore, *Atomic Energy Levels*, Natl. Bur. Std. Circ. No. 467 (U. S. GPO, Washington, D. C., 1952).

[10]See, for example, Y. Toyozawa, J. Lumines. 1/2, 732 (1970).

[11]R. H. Silsbee and D. B. Fichten, Rev. Mod. Phys. 36, 432 (1964).

[12]Thomas H. Keil, Phys. Rev. 140, A601 (1965).